JPn
Neuroscience
The Journal of Physiology

Differential signalling and glutamate receptor compositions in the OFF bipolar cell types in the mouse retina

Tomomi Ichinose[1,2] and Chase B. Hellmer[1]

[1] *Department of Anatomy and Cell Biology, Wayne State University School of Medicine, Detroit, MI 48201, USA*
[2] *Department of Ophthalmology, Wayne State University School of Medicine, Detroit, MI 48201, USA*

Key points

- Using whole-cell clamp methods, we characterized the temporal coding in each type of OFF bipolar cell.
- We found that type 2 and 3a cells are transient, type 1 and 4 cells are sustained, and type 3b cells are intermediate.
- The light-evoked excitatory postsynaptic potentials in some types were rectified, suggesting that they provide inputs to the non-linear ganglion cells.
- Visual signalling from the photoreceptors was mediated exclusively through the kainate receptors in the transient OFF bipolar cells, whereas both kainate and AMPA receptors contributed in the other cells.
- This study demonstrates, for the first time, that parallel visual encoding starts at the OFF bipolar cells in a type-specific manner.

Abstract The retina is the entrance to the visual system, which receives various kinds of image signals and forms multiple encoding pathways. The second-order retinal neurons, the bipolar cells, are thought to initiate multiple neural streams by encoding various visual signals in different types of cells. However, the functions of each bipolar cell type have not been fully understood. We investigated whether OFF bipolar cells encode visual signals in a type-dependent manner. We recorded the changes in the bipolar cell voltage in response to two input functions: step and sinusoidal light stimuli. Type 1 and 4 OFF bipolar cells were sustained cells and responded to sinusoidal stimuli over a broad range of frequencies. Type 2 and 3a cells were transient and exhibited band-pass filtering. Type 3b cells were in the middle of these two groups. The distinct temporal responses might be attributed to different types of glutamate receptors. We examined the AMPA and kainate glutamate receptor composition in each bipolar cell type. The light responses in the transient OFF bipolar cells were exclusively mediated by kainate receptors. Although the kainate receptors mediated the light responses in the sustained cells, the AMPA receptors also mediated a portion of the responses in sustained cells. Furthermore, we found that some types of cells were rectified more than other types. Taken together, we found that the OFF bipolar cells encode diverse temporal image signals in a type-dependent manner, confirming that each type of OFF bipolar cell initiates diverse temporal visual processing in parallel.

(Received 18 August 2015; accepted after revision 4 November 2015; first published online 10 November 2015)
Corresponding author T. Ichinose: Dept. of Anatomy and Cell Biology, Ophthalmology, Wayne State University School of Medicine, 540 E. Canfield, Detroit, MI 48201, USA. Email: tichinos@med.wayne.edu

Abbreviations ChAT, choline acetyltransferase; INL, inner nuclear layer; IPL, inner plexiform layer; L-EPSCs, light-evoked excitatory postsynaptic currents; L-EPSPs, light-evoked excitatory postsynaptic potentials; Syt2b, synaptotagmin 2B.

DOI: 10.1113/JP271458

Introduction

The retina has two main functions: capturing visual inputs and encoding them into separate, feature-based neural streams such as motion or colour-coded pathways. Diverse neural streams start at the second-order neurons in the retina, the bipolar cells, which is indicated by the existence of morphological types (Boycott & Wässle, 1991; Euler & Wässle, 1995; Ghosh *et al.* 2004; Pignatelli & Strettoi, 2004) as well as the distinct physiological responses in different types of bipolar cells (Awatramani & Slaughter, 2000; DeVries, 2000; Wu *et al.* 2000; Pang *et al.* 2004; Wässle, 2004). Thirteen types of bipolar cells have been identified in the mouse retina (Helmstaedter *et al.* 2013; Ichinose *et al.* 2014) whose physiological profiles have not yet been fully understood.

OFF bipolar cells are subsets of retinal bipolar cells that depolarize to light offset. Five types have been morphologically identified in the mouse retina (Ghosh *et al.* 2004; Mataruga *et al.* 2007; Wässle *et al.* 2009). Recent studies have clarified the unique characteristics associated with each type. The type 1 cells mediate colour vision (Breuninger *et al.* 2011). Types 3a, 3b and 4 receive mixed inputs from the cones and rods (Mataruga *et al.* 2007; Haverkamp *et al.* 2008). Temporal coding was studied using imaging techniques and demonstrated that the OFF bipolar cells with mid-inner plexiform layer (IPL)-ramifying axon terminals are transient and generate spikes, whereas the border IPL-ramifying cells are sustained (Baden *et al.* 2013; Borghuis *et al.* 2013). However, the manner in which this scheme corresponds to the morphological types has not been demonstrated.

Furthermore, the glutamate receptor types that are present in the OFF bipolar cell types are still controversial. The AMPA and kainate glutamate receptors show differential kinetics and expression patterns in each type of OFF bipolar cell, resulting in distinct temporal responses in the ground squirrel retina (DeVries, 2000; Lindstrom *et al.* 2014). These receptors are also differentially expressed in distinct types of OFF bipolar cells in the mouse retina (Puller *et al.* 2013). However, recent studies indicate that kainate receptors exclusively mediate bipolar cell signalling in the mouse and the primate retinas, while claiming that there is no function for AMPA receptors (Borghuis *et al.* 2014; Puthussery *et al.* 2014). We revisited this question, as studies have not examined the contribution of these receptors to the light responses in individual OFF bipolar cell types.

We found that temporal coding occurred in a type-specific manner. We also found that both kainate and AMPA glutamate receptors mediate the light responses of the OFF bipolar cells.

Methods

Ethical approval

All animal procedures were approved by the Institutional Animal Care and Use Committee at Wayne State University (protocol no. A05-03-15). All necessary steps were taken to minimize animal suffering. The tissues were harvested immediately after the animal was killed by CO_2 inhalation and bilateral pneumothorax.

Retinal preparation

The experimental techniques were similar to previously described methods (Ichinose & Lukasiewicz, 2012; Ichinose *et al.* 2014). Briefly, the mice (4–8 weeks old; male, C57BL/6J strain; Jackson Laboratory, Bar Harbor, ME, USA) were dark-adapted overnight and then killed. Using a dissecting microscope, the retina was isolated and cut into slice preparations (250 μm thick). Only the dorsal retina was used. All procedures were performed in dark-adapted conditions.

Whole-cell recordings

Whole-cell patch recordings were made from the bipolar cell somas in the retinal slices by viewing them with an upright microscope (Slicescope Pro 2000, Scientifica, Uckfield, East Sussex, UK) equipped with a CCD camera (Retiga-2000R, Q-Imaging, Surrey, BC, Canada). The light-evoked postsynaptic potentials and currents (L-EPSPs and L-EPSCs) were recorded at the resting membrane potential and at the equilibrium potential for chloride ions (E_{Cl}; −60 mV), respectively. All recordings were performed at 30–34°C. The liquid junction potentials were corrected after each recording. The electrodes were pulled from borosilicate glass (1B150F-4; WPI, Sarasota, FL, USA) with a P1000 Puller (Sutter Instruments, Novato, CA, USA) and had resistances of 7–11 MΩ. Clampex and Multi Clamp 700B (Molecular Devices, Sunnyvale, CA, USA) were used to generate the waveforms, acquire the data, and control LED light stimuli (Cool LED, Andover, UK). The data were digitized and stored on a personal computer using Axon Digidata 1440A (Molecular Devices). The responses were filtered at 2 kHz with the four-pole Bessel filter on the Multiclamp 700B and sampled at 2–5 kHz.

Solution and drugs

The retinal dissections were performed in Hepes-buffered extracellular solution containing the following (in mM): 115 NaCl, 2.5 KCl, 2.5 $CaCl_2$, 1.0 $MgCl_2$, 10 Hepes, and

28 glucose, adjusted to pH 7.4 with NaOH. Physiological recordings were performed in Ames' medium buffered with $NaHCO_3$ (Sigma, St Louis, MO, USA) and bubbled with 95% O_2 and 5% CO_2; the pH was 7.4 at 30–33°C. The intracellular solution contained the following (in mM): 111 potassium gluconate, 1.0 $CaCl_2$, 10 Hepes, 1.1 EGTA, 10 NaCl, 1.0 $MgCl_2$, 5 ATP-Mg, and 1.0 GTP-Na, adjusted to pH 7.2 with KOH. The potassium gluconate was replaced with caesium gluconate for the recording in voltage-clamp mode.

A cocktail of inhibitory receptor antagonists, including a glycine receptor antagonist, strychnine (1 μM, Sigma), a $GABA_A$ receptor antagonist, (−)-bicuculline methobromide (50 μM; Axxora, Farmingdale, NY, USA), and a $GABA_C$ receptor antagonist, TPMPA (R & D Systems, Minneapolis, MN, USA) (50 μM), were bath applied throughout all recordings to suppress the network effect. The glutamate receptor subsets were examined using ACET, GYKI52466, and GYKI53655 (R&D Systems). After the control light responses were recorded, an AMPA receptor antagonist (30 μM GYKI52466 or 50 μM GYKI53655; no differences were observed between two GYKIs. We used two forms of GYKIs to verify AMPA receptor blockade.) was bath applied. After GYKI was washed out, the kainate receptor antagonist (1 μM ACET) was applied in the same cell recording.

Light stimulation

Green light (500 nm) was projected through a ×60 objective lens onto the photoreceptors in the vicinity of the recorded bipolar cells with a diameter of 100 μm, which is slightly larger than the size of the receptive field centre for a bipolar cell (Berntson & Taylor, 2000; Borghuis *et al.* 2013). The preparations were adapted to background light at the rod-saturated level, 4.35×10^4 photons μm^{-2} s^{-1}. Step-light (30–60% Weber contrast) and sinusoidal light of various frequencies (0.3, 1, 3, 6, 10 and 20 Hz, 30–60% Michelson contrast) were sequentially projected (Ichinose *et al.* 2014). For the pharmacological experiments, all of the frequencies of the sinusoidal patterns (0.15, 0.6, 1, 2.5, 6, 9, 15 and 21 Hz) were applied simultaneously (Ichinose *et al.* 2014).

Morphological identification

A fluorescent dye, sulforhodamine B (0.005%, Sigma), and Neurobiotin (0.5%, Vector Labs, Burlingame, CA, USA) were included in the pipette. The sulforhodamine B images were captured after each recording. Then, the slice preparation was fixed with 4% paraformaldehyde for 30 min at room temperature; incubated with streptavidin-conjugated Alexa 488 (1:200, Life Technologies, Thermo Fisher Scientific, Waltham, MA, USA), an anti-synaptotagmin 2B antibody (Syt2b, 1:200, znp-1, ZIRC, Eugene, OR, USA), and an anti-choline acetyltransferase (ChAT) antibody (1:200, AB144P, Millipore, Billerica, MA, USA) overnight; and then with a secondary antibody for 2 h at room temperature. In some preparations, HCN4 (1:200, 75–150, NeuroMab, Davis, CA, USA) or PKARIIβ (1:3000, 610625, BD Biosciences, Franklin Lakes, NJ, USA) antibodies were used to confirm the type 3a or 3b cells. The preparation was viewed and the images were captured using a confocal microscope (TCS SP2 or SP8, Leica, Wetzlar, Germany).

The success rate of the Neurobiotin staining was 56% due to occasional accidental mishandling, such as the detachment of the retinal sections from the supporting filter paper or a lack of Neurobiotin staining for unknown reasons. We also filled the pipette with sulforhodamine B (100% success rate) to characterize the cells that were not labelled with Neurobiotin by measuring the IPL depth of their axon terminals and their patterns.

The image analysis was performed using AutoQuant X3 and the Image-Pro Premier 3D software (Media Cybernetics, Rockville, MD, USA). The image stacks captured by confocal microscopy were usually not aligned because the retinal slices were more or less tilted. Using 3-D analysis tools, the ChAT bands in image stacks were aligned, and then the Neurobiotin-filled bipolar cells were analysed. The widths of the axon terminals were measured at the widest point, which was determined by rotating the image. The initial branching point and the axon terminal branches were plotted in a 2-D graph for the individual OFF bipolar cells. The IPL depth was defined as 0% at the border of the inner nuclear layer (INL)/IPL and as 100% at the border of the IPL/ganglion cell layer. To determine the colocalization of the Neurobiotin labelling with the synaptotagmin 2B (Syt2b) staining, we analysed both images from multiple angles using the 3-D analysis tools.

Data analysis

For the step pulse light-evoked L-EPSPs, we measured the amplitude and time course of the offset light responses using Clampfit (Molecular Devices). We measured the peak amplitude from the baseline potential (before light onset) as the offset response (Fig. 2*D*). Also, we measured the time from the peak response to the amplitude at 37% of the peak (T-37). T-37 is small in transient cells, and large in sustained cells. For the sinusoidal responses, the amplitude (mV) was measured by fast Fourier transform (FFT) analysis using MatLab (MathWorks, Natick, MA, USA). The trough-to-trough amplitudes of the L-EPSPs were normalized to the maximum response in each cell and converted to the decibel (dB) scale. The cut-off responses were −3 dB of the maximal response. If the responses were a band-pass filtering feature, the attenuation plot crosses the −3 dB line (shown in orange in Fig. 3 graphs) twice, lower cut-off (f_1) and higher cut-off (f_2). If the

response was a low-pass filtering feature, we extrapolated the attenuation curve to lower frequencies, up to 0.01 Hz, to estimate the f_1 value. The unit of the bandwidth (BW) is an octave, which is calculated by BW $= \log_2(f_2/f_1)$. The '10 Hz attenuation' was the attenuation level at a 10 Hz frequency. Rectification was calculated by measuring the amplitudes of the baseline membrane potential to the trough (b) and the baseline to the peak of sinusoidal responses (a), and used the equation: Response modulation $= -b/(a - b) \times 100$ (Borghuis *et al.* 2013). Lower values show more response modulation by rectification (Fig. 4*D*). For the pharmacological experiments, the L-EPSC amplitude of offset responses and the amplitude of the sinusoidal L-EPSPs at 1 Hz were analysed.

Statistics

The values are presented as the means ± SEM. An unpaired t test, a one-way ANOVA test, and *post hoc* tests were conducted and the differences were considered significant if $P < 0.05$.

Results

Five types of OFF bipolar cells

Whole cell recordings were performed from 80 OFF bipolar cells. We recorded the light-evoked excitatory postsynaptic potentials (L-EPSPs) or currents (L-EPSCs) in response to either step-light stimuli or sinusoidal light stimuli. We used a cocktail of inhibitory receptor blockers to isolate the visual signals from the photoreceptors to the OFF bipolar cells. The types were identified by the axon terminal ramification patterns in the IPL (Ghosh *et al.* 2004; Wässle *et al.* 2009). We included Neurobiotin in the recording pipettes, which enabled us to characterize the axon terminals and identify the types of recorded cells by post-staining with streptavidin and other antibodies. We also filled the pipette with sulforhodamine B (100% success rate) to characterize the cell immediately after the physiological recordings were complete.

In response to a step-light stimulation, the L-EPSPs from the type 1 OFF bipolar cells were sustained (Fig. 1*A*). Their axon terminals ramified in the outer part of the IPL between the INL/IPL border and the OFF ChAT band (Fig. 1*A*). The type 2 cells were transient with a prominent transient component at the onset and offset of the light stimulation (Fig. 1*B*). The type 2 cells also ramified in the same sub-lamina as the type 1 cells (Fig. 2*A*). However, their axon terminals were more compact (Fig. 2*B*) and colocalized with Syt2b (Fig. 1*B*). Thus, we distinguished these two types by the Syt2b staining and axon terminal ramification patterns: the type 1 cells were thin and wider, whereas the type 2 cells were compact (Fig. 2).

The type 3 OFF bipolar cells were characterized as having axon terminals ramified below the OFF ChAT band (Figs 1*C* and *D*, and 2*A*). An immunohistochemical study shows that these cells can be further divided into two subsets, types 3a and 3b (Mataruga *et al.* 2007). We detected the two subsets based on their physiological characteristics. One subset of type 3 cells was transient (Fig. 1*C*), whereas another subset was more sustained (Fig. 1*D*). The Neurobiotin images did not distinguish the two subsets because their IPL ramifications and widths were similar (Fig. 2*A* and *B*). However, there are a few reasons why the transient and sustained type 3 cells were types 3a and 3b cells, respectively. First, three of the transient and one of the sustained type 3 cells colocalized with the HCN4 and PKARIIβ antibodies, respectively (Fig. 1*Cc* and *Dc*). Second, the transient type 3 cells, including the HCN4-positive cells, exhibited voltage-gated Na^+ currents, whereas the sustained type 3 cells, including the PKARIIβ-positive cell, did not (authors' unpublished observations). Therefore, we concluded that the transient and more sustained cells that we detected were the type 3a and 3b bipolar cells, respectively.

The type 4 cells were sustained and exhibited extensive branching patterns throughout the OFF sublaminae (Figs 1*E*, and 2*A* and *B*).

We analysed the properties of the step light-evoked L-EPSPs at the offset of the light stimulus in each type of OFF bipolar cell. The amplitude and decay phase time (T-37) were measured and shown in Fig. 2*D* and *C*, respectively. Types 1 and 4 were sustained cells with a significantly higher T-37 than the other three types ($P < 0.05$, unpaired t test) (Figs 1 and 2*C*). Moreover, the type 3a cells were more transient than the type 2 and 3b cells ($P < 0.05$, unpaired t test) (Figs 1 and 2*C*). The peak L-EPSP amplitudes were higher in the type 2, 3a and 3b cells than in the other types ($P < 0.05$, one-way ANOVA, Fig. 2*D*). Taken together, we found that types 1 and 4 are sustained cells and types 2 and 3a are transient cells. The type 3b cells showed transient responses; however, we categorized them as 'intermediate' because of their responses to the sinusoidal light stimuli (details below).

The resting membrane potentials were measured in the light-adapted conditions at the level of rod saturation (Methods) (Fig. 2*E*). The type 1, 2 and 4 cells were relatively more depolarized than the other types of cells. On average, the type 3a and 3b cells were more hyperpolarized than the other types of cells. In particular, these cells were significantly more hyperpolarized than the type 4 cells ($P < 0.05$).

Temporal analysis of the L-EPSPs

To further characterize the temporal encoding in the OFF bipolar cells, we used sinusoidal light stimuli with

a range of frequencies. The sinusoidal stimuli were projected with either individual frequencies or a sum of all frequencies (Ichinose *et al.* 2014). Similar responses were obtained with these methods. The L-EPSPs were different, depending on the OFF bipolar cell types (Fig. 3).

The temporal tuning corresponded to the transient/sustained nature of the cell. The sustained OFF bipolar cells exhibited a wider bandwidth and lower 10 Hz attenuation, and the transient cells exhibited the opposite effect (Fig. 4*A* and *B*). The type 3b cells exhibited a middle range of temporal tuning in response to step light stimuli; however, they responded to the sinusoidal stimuli with wider bandwidths and lower 10 Hz attenuation, similar to the sustained cells (Figs 3*D*, and 4*A* and *B*). Therefore, we consider that the type 3b have in-between transient–sustained properties. Both the type 2 and 3a cells showed band-pass filtering features (Figs 3*B* and *C*, and 4*A* and *B*). Interestingly, the type 2 cells tuned to a lower frequency than the type 3a cells ($P < 0.05$, unpaired, two tailed t test) (Fig. 4*C*), suggesting that these OFF bipolar cells provide distinct temporal tuning pathways. Spiking was observed in the type 3a cells at 0.3 Hz ($n = 4$, 3a cells, only one cell was included in the panels in Fig. 3*C*). When stimulated by the sum of the sine waves, they did not generate spikes. However, this might cause diverse responses in the type 3a cells at low frequencies (Fig. 3*C* panels). Therefore, we divided the five types into three groups: the type 1 and 4 cells were sustained and low temporal tuning, types 2 and 3a were transient and high temporal tuning, and type 3b was semi-transient and low temporal tuning.

Bipolar cells provide synaptic inputs to ganglion cells. The bipolar cell outputs are rectified, resulting in a non-linear spatial summation in many types of ganglion

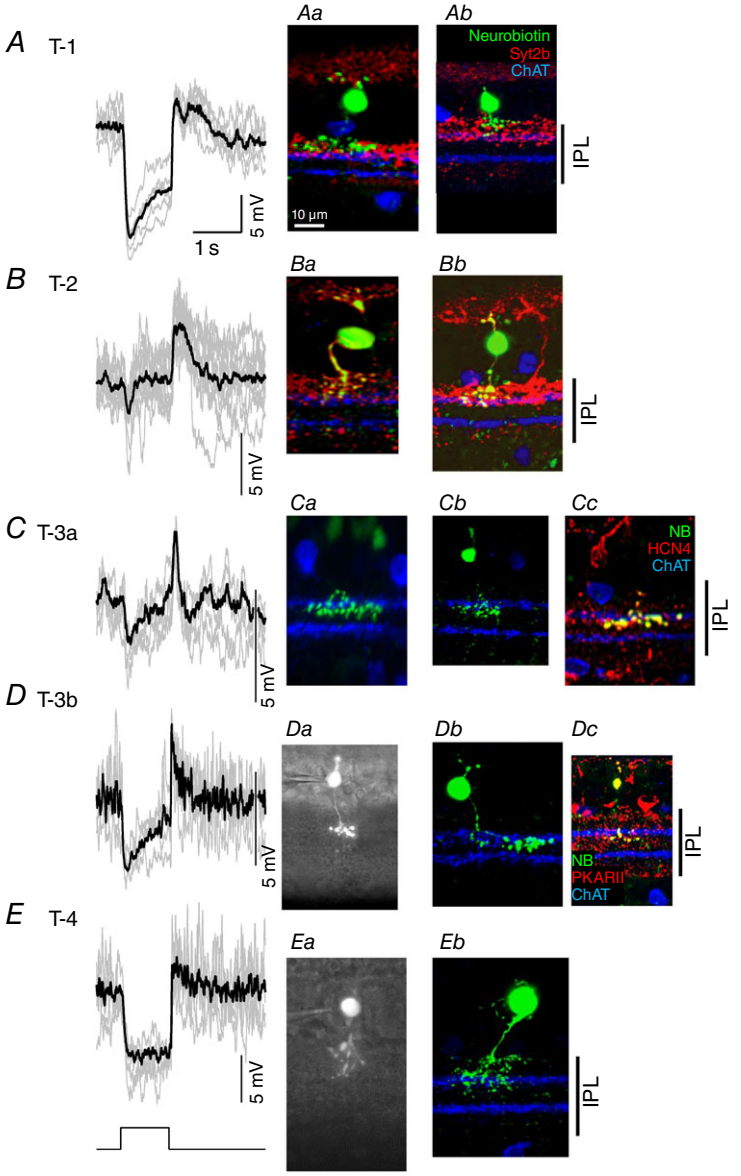

Figure 1. L-EPSPs and images of the five types of OFF bipolar cells
A, the L-EPSPs in response to the step-light stimuli were sustained in a type 1 OFF bipolar cell. Individual L-EPSPs (grey) and an averaged L-EPSP (black) are overlaid. *Aa*, a confocal microscopy image of the recorded cell. *Ab*, another type 1 cell. Type 1 was verified by axon terminal ramification in the outer IPL and the lack of colocalization with synaptotagmin 2B (Syt2b). *B*, the L-EPSPs in a type 2 OFF bipolar cell were transient. *Ba*, morphology of the cell from which the L-EPSPs were recorded. Type 2 cells were identified by their axon terminal ramification in the outer IPL and Syt2b colocalization, which is shown as yellow axon terminals. *Bb*, another type 2 cell. *C*, the L-EPSPs in a type 3a cell were transient. *Ca*, morphology of the cell from which the L-EPSPs were recorded. The axon terminals of the recorded cell ramified below the OFF ChAT band. *Cb*, another type 3a cell. *Cc*, HCN4 colocalized with the transient type 3 cell, confirming that these cells are type 3a. *D*, the L-EPSPs in type 3b cells were more sustained (at the light onset) and the decay phase of offset responses was slower than those of type 3a cells (see Fig. 2). *Da*, a sulforhodamine image of the recorded cell. The axon terminals of the type 3b cells ramify similar to type 3a cells. *Db*, another type 3b cell. *Dc*, a cell of this type colocalized with PKARIIβ, confirming that these cells are type 3b. *E*, the L-EPSPs in the type 4 cells were sustained. *Ea*, a sulforhodamine image of the recorded cell. The type 4 cells were distinguished from the other OFF bipolar cells by the ramification of their terminals throughout the OFF sublaminae. *Eb*, a confocal image of a type 4 cell. The terminals ramified both above and below the OFF ChAT band. NB: Neurobiotin.

cell receptive field centres (Baccus *et al.* 2008; Borghuis *et al.* 2013). We analysed how the OFF bipolar cell light responses were rectified at various temporal frequencies using the L-EPSPs in response to individual sinusoidal light stimuli (the type 3a cells were not included because $n = 1$). The L-EPSPs were scarcely rectified at 0.3 Hz of sinusoidal stimulation, showing that the response modulation was approximately 50% (Figs 3 and 4*D*). Rectification was recognized across all types at higher frequency stimulations. The differences between types were observed at 1–6 Hz; the type 2 and 4 cells were relatively more rectified than the other types. These types may provide greater input to the non-linear ganglion cells. Collectively, these results suggested that the OFF bipolar cells rectified at higher frequencies in a type-dependent manner.

Glutamate receptors mediate the visual signals

The distinct temporal features of the OFF bipolar cells might arise from two types of glutamate receptors: AMPA and kainate. Recent evidence suggested that the functional glutamate receptors in the OFF bipolar cells are exclusively kainate receptors (Borghuis *et al.* 2014; Puthussery *et al.* 2014). However, it has not been demonstrated how the light-evoked responses in the individual types of OFF bipolar cells were mediated by these receptors. We tested the effects of GYKI (an AMPA receptor antagonist) as well as ACET (a kainate receptor antagonist) on the step light-evoked L-EPSCs or sinusoidal light-evoked L-EPSPs. The L-EPSPs were analysed in response to 1 Hz sinusoidal stimulation because they might resemble the 1-s step stimuli. The effects of GYKI/ACET on the L-EPSCs and L-EPSPs were similar among all types, suggesting that these receptor antagonists operated at the postsynaptic level. The pharmacological experiments were conducted in the presence of inhibitory receptor antagonists to avoid evoking any network effect. We applied GYKI first, washed it out, and then ACET was applied to the same cells. For some cells, we applied these inhibitors in the opposite order (ACET then GYKI), and observed similar effects (type 2, $n = 1$: type 3a, $n = 2$: type 4, $n = 1$).

Both GYKI and ACET reduced the light responses in a subset of the OFF bipolar cells. The light responses in the type 1 cells were primarily mediated by AMPA receptors (Fig. 5*A*). ACET also reduced a small portion of the light responses (Fig. 5*A*, *F* and *G*). In contrast, ACET abolished

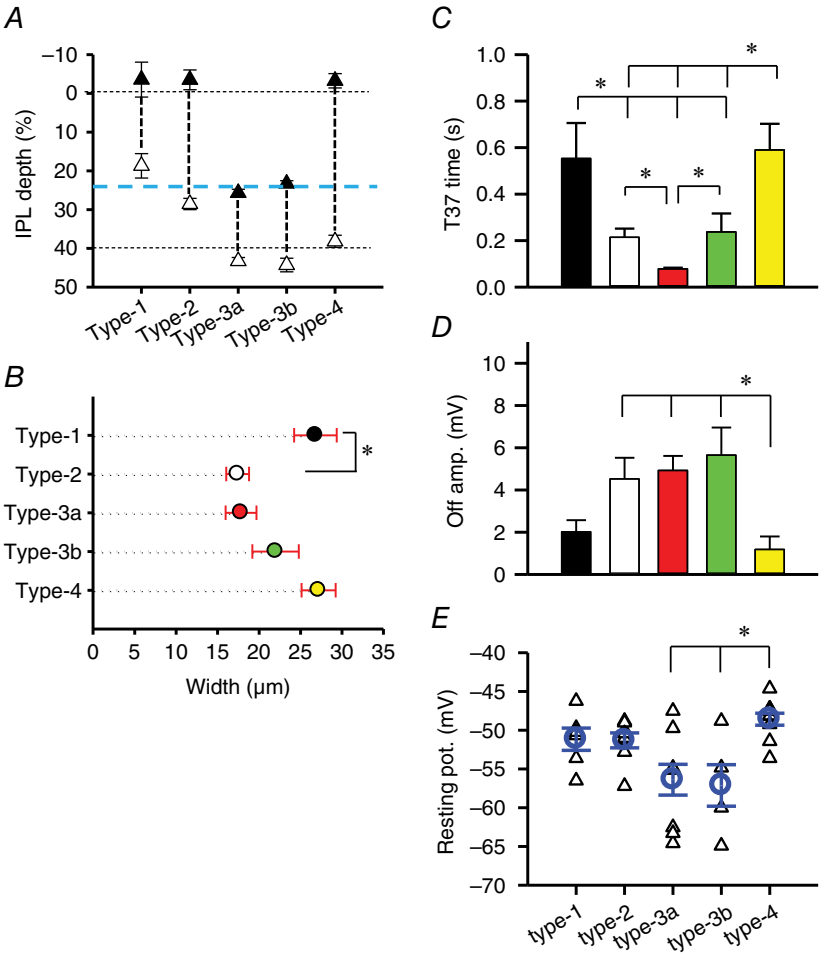

Figure 2. Analysis of morphology and L-EPSPs in response to the step light stimuli
A, ranges of the axon terminal ramification in the IPL. The black triangles show the initial branching point of the axon terminals and open triangles show the innermost point of the terminals. The horizontal dotted lines show borders of the INL/IPL (0%) and the ON/OFF sublaminae (40%). The blue dashed line indicates the OFF ChAT band at 24% (Ichinose *et al.* 2014). *B*, the axon terminals were measured at the widest points of each type of OFF bipolar cell. The type 1 cell terminals were significantly wider than the type 2 terminals ($P < 0.05$). The numbers of each type of cells used in the morphological analysis were 5 (type 1), 12 (type 2), 11 (type 3a), 4 (type 3b), and 6 (type 4). *C*, T-37 at the light offset from each type of OFF bipolar cell. Type 3a exhibited the shortest offset responses. *D*, the amplitudes of the L-EPSPs at the light offset. *E*, the resting membrane potentials (V_m) in each type of OFF bipolar cell. The triangles represent the V_m of individual cells. The circles and error bars show the average and SEM values. The numbers of recorded cells were 6 (type 1), 11 (type 2), 11 (type 3a), 4 (type 3b) and 10 (type 4). *The type 4 cells were significantly more depolarized than the type 3a and type 3b cells ($P < 0.05$, one-way ANOVA).

almost all of the responses in the type 2 and 3a cells (Fig. 5*B*, *C*, *F* and *G*). The light responses in the type 3b cells were mainly mediated by kainate; however, GYKI also reduced their light responses (Fig. 5*D*, *F* and *G*). The light responses in the type 4 cells were mediated by both AMPA and kainate receptors (Fig. 5*E*–*G*). Taken together, these results indicate that kainate receptors mediated the light responses in all types of OFF bipolar cells. However, AMPA receptors also mediated the light responses, particularly in the sustained OFF bipolar cells.

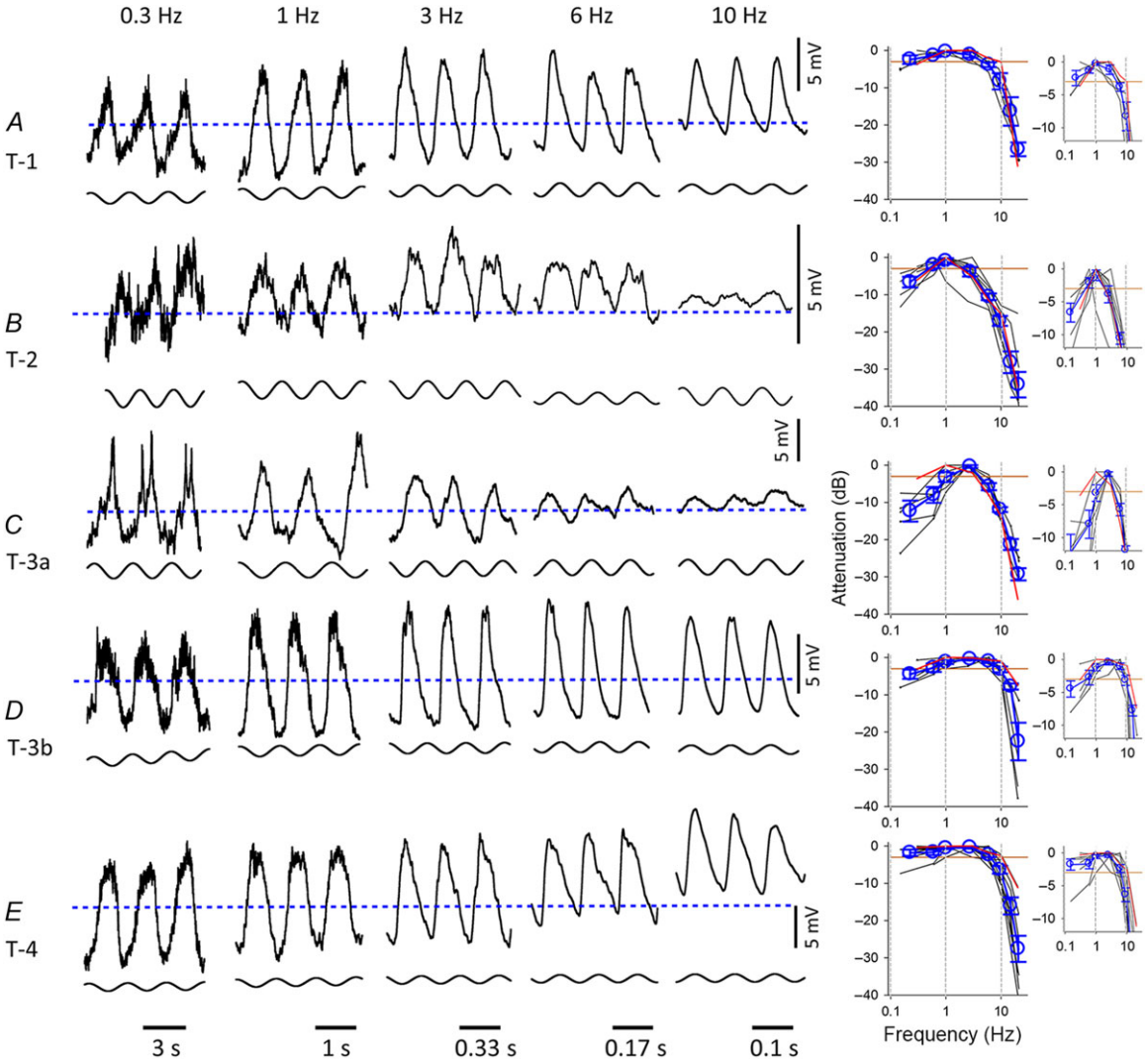

Figure 3. L-EPSPs in response to the sinusoidal light stimuli
A, L-EPSPs in a type 1 OFF bipolar cell in response to individual sinusoidal light stimuli. The baseline level for all five traces is indicated by a blue dashed line. The mean levels of L-EPSPs were depolarized in some conditions, suggesting that the L-EPSPs were rectified. The graph shows the attenuation level from the peak amplitude of the L-EPSPs in response to either individual sinusoidal or mixed sinusoidal light stimuli. Each line represents the individual cell responses, and the red line indicates the attenuation of the representative L-EPSPs in the panels. The averages and SEM were plotted in blue. Because the two protocols evoked L-EPSPs at slightly different frequencies, we consolidated some of the similar frequency responses and plotted the mid-point (0.15 and 0.3 Hz responses at 0.225 Hz: 2.5 and 3 Hz responses at 2.75 Hz: 9 and 10 Hz at 9.5 Hz: and 20 and 21 Hz responses at 20.5 Hz). The small graphs show the same data sets with expanded lower attenuation levels. These graphs show the low and high cutoff levels more clearly. *B*, type 2 cells. *C*, type 3a cells. *D*, type 3b cells. *E*, type 4 cells. The numbers of cells included in the right-hand panels were as follows. *A*: $n = 3$ for the individual sine waves (SW), $n = 2$ for the sum of sign waves (S-SW); *B*: $n = 3$ (SW), $n = 5$ (S-SW); *C*: $n = 1$ (SW), $n = 5$ (S-SW); *D*: $n = 4$ (SW), $n = 2$ (S-SW); *E*: $n = 5$ (SW), $n = 5$ (S-SW). The orange lines in the summary graphs indicate the −3 dB cutoff points and the two dotted vertical lines indicate 1 and 10 Hz. The horizontal lines at the bottom of traces indicate the length of one cycle and the time for each frequency.

Discussion

OFF bipolar cell visual encoding

In the present study, we demonstrated that the OFF bipolar cells encode diverse temporal visual signals in a type-specific manner. Previously, we presented the type-specific temporal encoding in ON bipolar cells (Ichinose *et al.* 2014). Taken together, each morphological type of cone bipolar cell plays a role in temporal coding. Differences were observed in the sustained cells. In ON bipolar cells, the sustained cells only respond to a low frequency light stimulus, whereas in the OFF bipolar cells, the sustained cells responded to broader ranges of frequencies than their transient cell counterparts (Fig. 4*A*). Additionally, the temporal tuning in the ON bipolar cells was more diverse across all frequencies compared to the OFF cells.

It is generally understood that the dendrites and axons of the transient cells from many species ramify in the mid-IPL of the retina, whereas the processes of the sustained cells ramify at the border of the IPL (Awatramani & Slaughter, 2000; Ichinose *et al.* 2005; Euler *et al.* 2014). Recent studies demonstrate that the calcium signals and glutamate release from the bipolar cell axon terminals follow this rule (Baden *et al.* 2013; Borghuis *et al.* 2013). For the most part, our results also follow this rule; however, we found that the transient and sustained cells are rather mingled in the IPL OFF sublaminae. The type 1 axon terminals widely

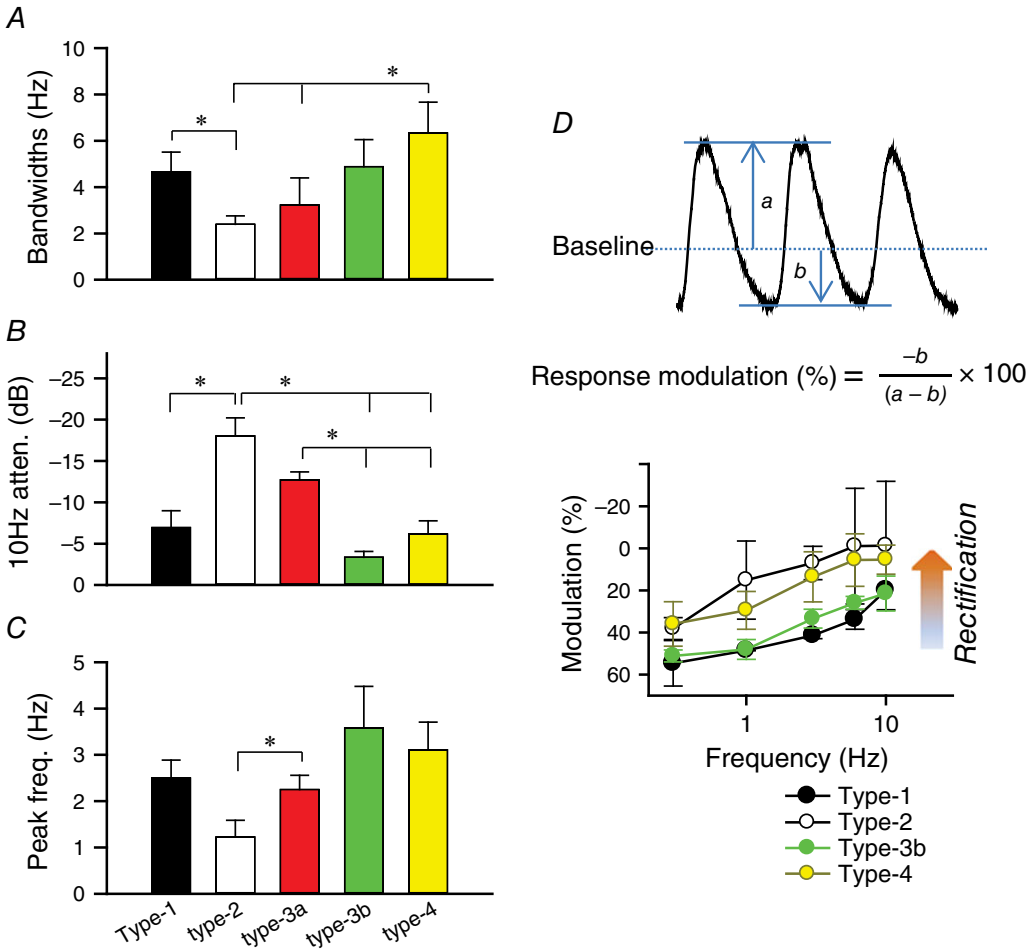

Figure 4. Summary of the L-EPSP parameters
A, bandwidths derived from the sinusoidal light stimuli. *B*, the 10 Hz attenuation derived from the sinusoidal light stimuli. *C*, peak frequency of the sinusoidal responses. The numbers of recorded cells were 5 (type 1), 8 (type 2), 6 (type 3a), 6 (type 3b) and 10 (type 4). The asterisk indicates a significant difference between the two groups ($P < 0.05$). *D*, the percentage of the response modulation was calculated using the equation (*a*: baseline to peak amplitude/*b*: baseline to trough amplitude) and plotted as a function of the sinusoidal frequencies. Fifty per cent indicates that there was no rectification, while a lower % shows more rectification. The numbers of recorded cells were 3 (type 1), 3 (type 2), 4 (type 3b) and 5 (type 4). Significant differences were observed between the type 1 and type 4 cells (1 Hz, $P < 0.05$, unpaired *t* test for all combinations reported), type 1 and type 2 cells (3 Hz, $P < 0.05$), type 2 and type 3 cells (3 Hz, $P < 0.05$), and type 1 and type 4 cells (6 Hz, $P < 0.05$, unpaired *t* test).

stratify near the outer border of the IPL and respond to light in a sustained manner. The ramification of the axon terminals of the type 2 cells was very similar to the type 1 cells; however, the type 2 cells exhibited more transient responses. Additionally, the type 3b cells ramify similar to the type 3a cells; however, the type 3b cells were more sustained compared to the type 3a cells. Furthermore, the type 4 cells ramify throughout the OFF sublaminae and exhibited a sustained response (Figs 1*E* and 2). Thus, sustained signalling might exist in the mid-IPL. Alternatively, the sustained visual signalling recorded in the soma of the type 4 cells could be converted to a more transient signal at the axon terminals in the mid-IPL by amacrine cell modulation or channel activity. Further

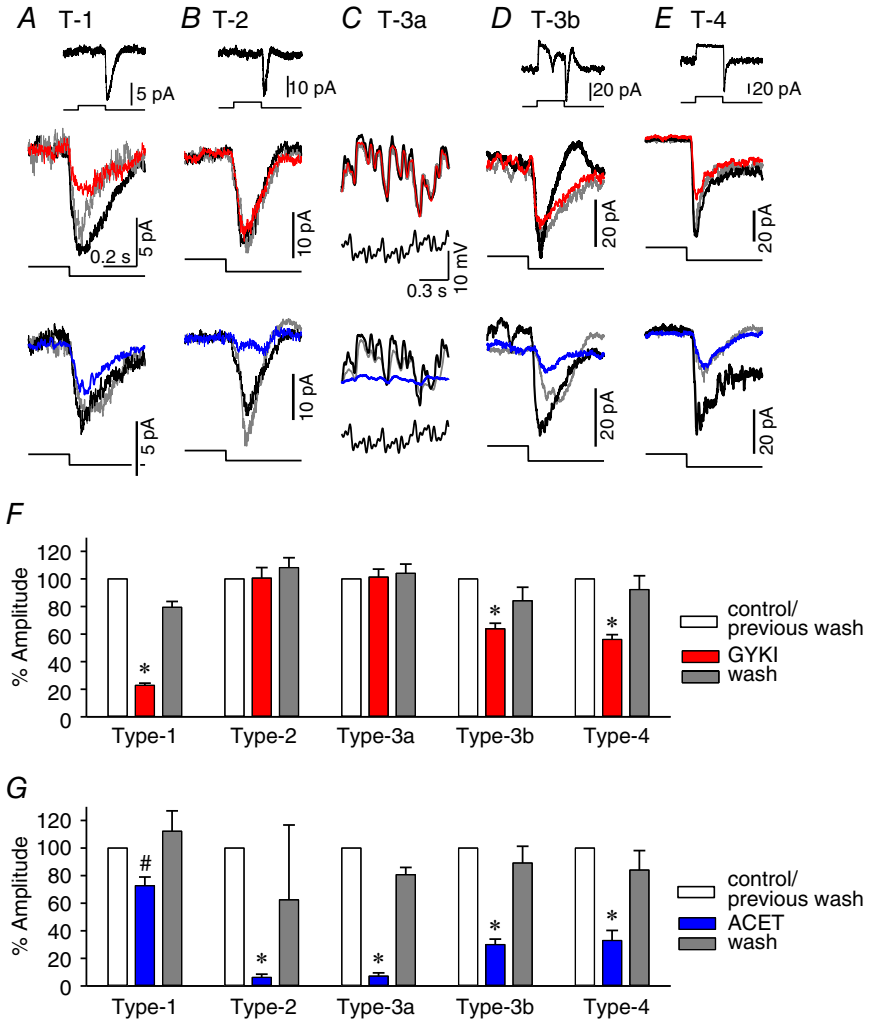

Figure 5. Both AMPA and kainate receptors contribute to the light responses of the OFF bipolar cells
A, L-EPSCs from a type 1 OFF bipolar cell (inset). The light-offset responses from the cell were magnified and displayed in the lower panels to show the pharmacological effects. The GYKI effects are shown in red, the ACET effects are shown in blue, and the responses after washout are shown in dark grey. In the type 1 cells, GYKI reduced the L-EPSCs. ACET also reduced the L-EPSCs. *B*, L-EPSCs from a type 2 OFF bipolar cell. GYKI did not affect the L-EPSCs while ACET almost completely abolished L-EPSCs. *C*, L-EPSPs in response to a mixed sine wave stimulus in a type 3a cell. GYKI did not change the L-EPSPs, while ACET abolished the response. *D*, L-EPSCs from a type 3b cell. GYKI reduced a portion of the L-EPSCs, while ACET reduced a majority of the L-EPSCs. *E*, L-EPSCs from a type 4 OFF bipolar cell. Both GYKI and ACET reduced the L-EPSCs. *F*, the peak amplitude was measured at the light offset from the steady-state light onset level. The summary graph shows the % changes in the amplitudes compared to the control responses. The GYKI response is shown in red, while the response after washout is shown in grey. *G*, the summary graph shows the % amplitude when ACET was applied (blue) and washed out (grey). *Statistical significance *vs.* the control ($P < 0.01$, paired *t* test), $^{\#}P < 0.05$, paired *t* test. The numbers of recorded cells were 4 (type 1), 8 (type 2), 8 (type 3a), 5 (type 3b) and 9 (type 4). A scale bar was included in each panel. The light stimuli were delivered for 1 s (inset).

studies are required to elucidate the detailed visual signal processing pathways.

We used background light at the rod saturated level (4.35×10^4 photons μm^{-2} s^{-1}) to isolate the cone signals. However, a previous report proposed that the rod inputs may be active in the guinea pig retina, even with high background light (Yin *et al.* 2006). In our conditions, we rarely observed L-EPSPs in the rod bipolar cells that receive synaptic inputs directly from the rod photoreceptors ($n = 20$), even after 30 min of light adaptation at this level. This might be attributed to the retinal preparations. We used isolated retinal slice preparations and Yin *et al.* used eye-cup preparations. The retinal epithelium layer had been removed in our preparations, which is critical for rod photoreceptor regeneration. Collectively, these results suggested that the light-evoked responses in our conditions were primarily from cone signalling.

Spiking activity was observed in the type 3a cells at a 0.3 Hz light stimulus ($n = 4$, Fig. 3*C*). This may be the Ca^{2+} spikes that were reported by Baden *et al.* (2013). The other possibility is that they are the Na^+ spikes described by Cui & Pan (2008), Saszik & DeVries (2012) and Baden *et al.* (2013). Consistent with previous reports, we recently detected Na^+ currents in type 3a cells (authors' unpublished observations). Spiking activity is probably one of the underlying mechanisms of the high temporal tuning in this type of cell.

We found that the light responses in the OFF bipolar cells were rectified in a type-dependent manner (Figs 3 and 4*D*). The non-linearity in some types of ganglion cells was attributed to either the photoreceptor to bipolar cell transmission (Schneeweis & Schnapf, 1999; Hennig *et al.* 2002) or to the bipolar cell to ganglion cell transmission (Baccus *et al.* 2008; Schwartz *et al.* 2012). Rectification in bipolar cells is a key underlying mechanism of non-linearity in ganglion cells (Demb *et al.* 2001; Borghuis *et al.* 2013). Our results indicate that the ganglion cells' non-linearity is already initiated at the soma of some OFF bipolar cells.

OFF bipolar cell glutamate receptors

The distinct temporal features of the OFF bipolar cells might arise from two types of glutamate receptors. Kainate and AMPA receptors mediate the OFF bipolar cell excitatory inputs in the ground squirrel retina, which are present in different types of OFF bipolar cells and shape temporal signalling (DeVries, 2000; Lindstrom *et al.* 2014). Kainate and AMPA receptors are also expressed in distinct types of OFF bipolar cells in the mouse retina (Puller *et al.* 2013); however, recent studies indicate that only the kainate receptors are functional in the mouse and primate retina (Borghuis *et al.* 2014; Puthussery *et al.* 2014).

We examined the contributions of the AMPA and kainate receptors to the temporal tuning in all types of OFF bipolar cells. Our results are consistent with Puller *et al.* (2013), who demonstrated that AMPA exclusively mediates the EPSCs in type 1 cells, kainate is exclusively responsible for the EPSCs in the type 2 and 3a cells, and both AMPA and kainate are equally expressed and mediate the EPSCs in the type 3b and 4 cells. Our pharmacological results match their findings, with the exception of the type 1 cells. GYKI reduced the light responses of the type 1 cells by 80%, but did not eliminate the response. In the same cells, ACET reduced a small portion of the response (Fig. 5*G*). Puller *et al.* (2013) used Sym2081, a kainate receptor agonist, whereas we used ACET, a potent kainate receptor antagonist, which might explain the different outcomes.

GYKI might hyperpolarize the horizontal cells, which increases the feedback to the cone photoreceptors and might affect the light responses in the OFF bipolar cells. This scenario may not have occurred in our conditions because GYKI did not change the membrane potentials (current clamp mode) or the baseline current (voltage clamp mode) ($n = 10$ OFF bipolar cells). This might be attributed to our conditions, using a small spot light stimulus (diameter 100 μm) and background light conditions at rod-saturated level. The spot of light minimally stimulates the horizontal cells and the background illumination reduces the changes in the membrane potential in horizontal cells in response to the GYKI application. We also demonstrated that the horizontal cells were not involved because ACET complemented the effect of GYKI on the light responses.

In our results, ACET mediated the light responses in all OFF bipolar cell types, which is consistent with the results of Borghuis *et al.* (2014). However, GYKI also reduced the responses in some types of OFF bipolar cells in our study. We found some discrepancies in the experimental conditions that might explain the different results. Borghuis *et al.* (2014) used L-2-amino-4-phosphonobutyric acid (L-AP4) to suppress the network effect whereas we used GABA and glycine receptor blockers. They used mice that were older (2–6 months) than those used in our study (1–2 months). Finally, the recording methods were different. We used single cell recordings from the bipolar cell somas, whereas they recorded from ganglion cells to detect the bipolar cell outputs. These discrepancies may explain the differences in our results.

AMPA receptors have been shown to quickly desensitize and mediate fast transmission (DeVries, 2000), whereas kainate receptors mediate transmission with diverse temporal properties (Lindstrom *et al.* 2014). These properties of kainate receptors are consistent with the diverse subunits (GluK 1–5) and auxiliary subunits (Neto1 and Neto2) that may determine the temporal kinetics

(Lindstrom *et al.* 2014; Zhang *et al.* 2014). In our study, the AMPA receptors were expressed in the sustained cells (types 1, 3b and 4), while kainate exclusively mediated transient cell visual signalling (types 2 and 3a). The expression of the different kainate subunits may differ among the OFF bipolar cell types; however, further studies are needed to elucidate the functional significance of the AMPA and kainate receptors in the OFF bipolar cells in the mouse retina.

In conclusion, we characterized the temporal coding in each type of OFF bipolar cell using whole-cell clamp methods. We found that the type 2 and 3a cells are transient cells, types 1 and 4 are sustained cells, and the type 3b cells are intermediate cells. The transient cells were tuned to a particular frequency of visual signals, while the sustained cells responded to a broad frequency of light stimuli. Finally, the visual signals from the photoreceptors were exclusively transmitted through the kainate receptors in the transient OFF bipolar cells, whereas both the kainate and AMPA receptors contributed in the sustained cell types. Some types of L-EPSPs were rectified, suggesting that they provide inputs to the non-linear ganglion cells. This study demonstrates, for the first time, that parallel visual encoding in the mouse retina starts at OFF bipolar cells in a type-specific manner.

References

Awatramani GB & Slaughter MM (2000). Origin of transient and sustained responses in ganglion cells of the retina. *J Neurosci* **20**, 7087–7095.

Baccus SA, Olveczky BP, Manu M & Meister M (2008). A retinal circuit that computes object motion. *J Neurosci* **28**, 6807–6817.

Baden T, Berens P, Bethge M & Euler T (2013). Spikes in mammalian bipolar cells support temporal layering of the inner retina. *Curr Biol* **23**, 48–52.

Berntson A & Taylor WR (2000). Response characteristics and receptive field widths of on-bipolar cells in the mouse retina. *J Physiol* **524**, 879–889.

Borghuis BG, Looger LL, Tomita S & Demb JB (2014). Kainate receptors mediate signaling in both transient and sustained OFF bipolar cell pathways in mouse retina. *J Neurosci* **34**, 6128–6139.

Borghuis BG, Marvin JS, Looger LL & Demb JB (2013). Two-photon imaging of nonlinear glutamate release dynamics at bipolar cell synapses in the mouse retina. *J Neurosci* **33**, 10972–10985.

Boycott BB & Wässle H (1991). Morphological classification of bipolar cells of the primate retina. *Eur J Neurosci* **3**, 1069–1088.

Breuninger T, Puller C, Haverkamp S & Euler T (2011). Chromatic bipolar cell pathways in the mouse retina. *J Neurosci* **31**, 6504–6517.

Cui J & Pan ZH (2008). Two types of cone bipolar cells express voltage-gated Na^+ channels in the rat retina. *Vis Neurosci* **25**, 635–645.

Demb JB, Zaghloul K, Haarsma L & Sterling P (2001). Bipolar cells contribute to nonlinear spatial summation in the brisk-transient (Y) ganglion cell in mammalian retina. *J Neurosci* **21**, 7447–7454.

DeVries SH (2000). Bipolar cells use kainate and AMPA receptors to filter visual information into separate channels. *Neuron* **28**, 847–856.

Euler T, Haverkamp S, Schubert T & Baden T (2014). Retinal bipolar cells: elementary building blocks of vision. *Nat Rev Neurosci* **15**, 507–519.

Euler T & Wässle H (1995). Immunocytochemical identification of cone bipolar cells in the rat retina. *J Comp Neurol* **361**, 461–478.

Ghosh KK, Bujan S, Haverkamp S, Feigenspan A & Wässle H (2004). Types of bipolar cells in the mouse retina. *J Comp Neurol* **469**, 70–82.

Haverkamp S, Specht D, Majumdar S, Zaidi NF, Brandstatter JH, Wasco W, Wässle H & Tom Dieck S (2008). Type 4 OFF cone bipolar cells of the mouse retina express calsenilin and contact cones as well as rods. *J Comp Neurol* **507**, 1087–1101.

Helmstaedter M, Briggman KL, Turaga SC, Jain V, Seung HS & Denk W (2013). Connectomic reconstruction of the inner plexiform layer in the mouse retina. *Nature* **500**, 168–174.

Hennig MH, Funke K & Worgotter F (2002). The influence of different retinal subcircuits on the nonlinearity of ganglion cell behavior. *J Neurosci* **22**, 8726–8738.

Ichinose T, Fyk-Kolodziej B & Cohn J (2014). Roles of ON cone bipolar cell subtypes in temporal coding in the mouse retina. *J Neurosci* **34**, 8761–8771.

Ichinose T & Lukasiewicz PD (2012). The mode of retinal presynaptic inhibition switches with light intensity. *J Neurosci* **32**, 4360–4371.

Ichinose T, Shields CR & Lukasiewicz PD (2005). Sodium channels in transient retinal bipolar cells enhance visual responses in ganglion cells. *J Neurosci* **25**, 1856–1865.

Lindstrom SH, Ryan DG, Shi J & DeVries SH (2014). Kainate receptor subunit diversity underlying response diversity in retinal Off bipolar cells. *J Physiol* **592**, 1457–1477.

Mataruga A, Kremmer E & Muller F (2007). Type 3a and type 3b OFF cone bipolar cells provide for the alternative rod pathway in the mouse retina. *J Comp Neurol* **502**, 1123–1137.

Pang JJ, Gao F & Wu SM (2004). Light-evoked current responses in rod bipolar cells, cone depolarizing bipolar cells and AII amacrine cells in dark-adapted mouse retina. *J Physiol* **558**, 897–912.

Pignatelli V & Strettoi E (2004). Bipolar cells of the mouse retina: a gene gun, morphological study. *J Comp Neurol* **476**, 254–266.

Puller C, Ivanova E, Euler T, Haverkamp S & Schubert T (2013). OFF bipolar cells express distinct types of dendritic glutamate receptors in the mouse retina. *Neuroscience* **243**, 136–148.

Puthussery T, Percival KA, Venkataramani S, Gayet-Primo J, Grunert U & Taylor WR (2014). Kainate receptors mediate synaptic input to transient and sustained OFF visual pathways in primate retina. *J Neurosci* **34**, 7611–7621.

Saszik S & DeVries SH (2012). A mammalian retinal bipolar cell uses both graded changes in membrane voltage and all-or-nothing Na^+ spikes to encode light. *J Neurosci* **32**, 297–307.

Schneeweis DM & Schnapf JL (1999). The photovoltage of macaque cone photoreceptors: adaptation, noise, and kinetics. *J Neurosci* **19**, 1203–1216.

Schwartz GW, Okawa H, Dunn FA, Morgan JL, Kerschensteiner D, Wong RO & Rieke F (2012). The spatial structure of a nonlinear receptive field. *Nat Neurosci* **15**, 1572–1580.

Wässle H (2004). Parallel processing in the mammalian retina. *Nat Rev Neurosci* **5**, 747–757.

Wässle H, Puller C, Muller F & Haverkamp S (2009). Cone contacts, mosaics, and territories of bipolar cells in the mouse retina. *J Neurosci* **29**, 106–117.

Wu SM, Gao F & Maple BR (2000). Functional architecture of synapses in the inner retina: segregation of visual signals by stratification of bipolar cell axon terminals. *J Neurosci* **20**, 4462–4470.

Yin L, Smith RG, Sterling P & Brainard DH (2006). Chromatic properties of horizontal and ganglion cell responses follow a dual gradient in cone opsin expression. *J Neurosci* **26**, 12351–12361.

Zhang W, Devi SP, Tomita S & Howe JR (2014). Auxiliary proteins promote modal gating of AMPA- and kainate-type glutamate receptors. *Eur J Neurosci* **39**, 1138–1147.

Additional information

Competing interests

None declared.

Author contributions

Conception of the work: T.I. Acquisition, analysis and interpretation of data: T.I. and C.B.H. Drafting the manuscript and critically revising it for important intellectual content: T.I. and C.B.H. Approved the final version of the manuscript: T.I. and C.B.H. Agree to be accountable for all aspects of the work and ensure that questions related to the accuracy or integrity of any part of the work are appropriately investigated and resolved: T.I. and C.B.H. All persons designated as authors qualify for authorship, and all those who qualify for authorship are listed.

Funding

This work was supported by grants from the NIH (R01 EY020533), the Wayne State University Startup Fund and Research to Prevent Blindness (RPB).

Acknowledgements

We would like to thank Drs Pan and Fyk-Kolodziej for constructive comments on the paper manuscript. We also thank Dr Fyk-Kolodziej for assistance with the morphological analysis.